

Extensive validation of solar spectral irradiance meters at the World Radiation Center



V. Tatsiankou^{a,c,*}, K. Hinzer^a, H. Schriemer^a, S. Kazadzis^b, N. Kouremeti^b, J. Gröbner^b, R. Beal^c

^a University of Ottawa, SUNLAB, Ottawa, Ontario K1N 6N5, Canada

^b Physikalisch-Meteorologisches Observatorium Davos, World Radiation Center, Switzerland

^c Spectrafy Inc., Ottawa, Ontario K2P 0W7, Canada

ARTICLE INFO

Keywords:

Solar spectral irradiance meter
SolarSIM
Direct normal spectral irradiance
Aerosol optical depth
Total ozone column amount
Precipitable water vapor content
Solar resource assessment
Atmospheric parameterization

ABSTRACT

A comprehensive uncertainty analysis validates a Solar Spectral Irradiance Meter (SolarSIM) for accurately resolving the spectral and broadband direct normal irradiances (DNI), spectral aerosol optical depth (AOD), precipitable water vapour and atmospheric total column ozone amounts. The derivation of these parameters from four SolarSIMs were compared to reference instrumentation at the Physikalisch-Meteorologisches Observatorium Davos and World Radiation Center (PMOD/WRC) in Davos, Switzerland in September 2015. The SolarSIMs are the first instruments to ever simultaneously participate in the 12th WMO International Pyrheliometer Comparison, Fourth Filter Radiometer Comparison, and First Spectroradiometer Comparison. The SolarSIMs' DNI data were compared to the World Standard Group's PMO2 absolute cavity radiometer, with World Radiometric Reference factors ranging from 0.999674 to 0.994610 for the best and the worst performing devices, respectively. In addition, the SolarSIMs' spectral DNI data was compared against PMOD's Precision Spectral Radiometer. The mean difference of the spectral DNI was found to be less than 5% for wavelengths above 400 nm. The SolarSIMs' measurements of AOD data were compared against PMOD's Precision Filter Radiometer triad. The median AOD differences and their standard deviations were found to be 0.0046 ± 0.0044 , 0.0016 ± 0.0034 , 0.0018 ± 0.0026 , and 0.0041 ± 0.0022 for 368 nm, 412 nm, 500 nm, and 865 nm, respectively. The SolarSIMs' measurements of precipitable water vapour were compared against PMOD's Cimel CE318 sun photometer. The median difference and the corresponding standard deviation averaged 1 ± 0.2 mm for all SolarSIMs. Furthermore, the SolarSIMs' measurements of total column atmospheric ozone were compared against PMOD's Brewer MkIII spectrophotometer. The median difference and the corresponding standard deviation averaged 6 ± 7 DU for all SolarSIMs.

1. Introduction

For decades now, measurements of sunlight have been vital for solar energy research, atmospheric science, and weather forecasting applications. Broadband direct normal irradiance (DNI) measurements, for example, have been extensively used for solar resource assessment and calibration of satellite-derived irradiance data sets (AlYahya and Irfan, 2016; Cebecauer and Suri, 2016). More recently, with the advent of concentrating photovoltaic technologies, spectral DNI measurements became critical for performance analysis of solar modules with high efficiency multi-junction solar cells (Núñez et al., 2016; Araki and Yamaguchi, 2003). Besides the spectral and broadband irradiance data, direct sun observations can quantify the aerosol optical depth (AOD), precipitable water vapor (PWV) and total column ozone contents of the atmosphere. The aerosols and water vapor impact earth's radiation

budget and are key inputs into weather prediction models and climate studies (Holben et al., 2001; Liang et al., 2015; Karabatić et al., 2011), while the ozone layer is critical for protecting life on our planet, as it attenuates damaging ultraviolet radiation.

For over 50 years the Physikalisch-Meteorologisches Observatorium Davos and World Radiation Center (PMOD/WRC) in Davos, Switzerland has guaranteed the global homogenization of solar measurements by hosting quinquennial instrument inter-comparisons, such as the International Pyrheliometer Comparison (IPC) (Finsterle, 2016), the Filter Radiometer Comparison (FRC) (Kazadzis et al., 2016), and the Spectroradiometer Comparison (SRC) (Schmutz et al., 2016). A group of absolute cavity radiometers, known as the World Standard Group (WSG), is the manifestation of the World Radiometric Reference (WRR) with an estimated uncertainty to the International System of Units. The WRR is the world's primary standard for the DNI. During the IPC, the

* Corresponding author at: University of Ottawa, SUNLAB, Ottawa, Ontario K1N 6N5, Canada.
E-mail address: viktat.tatsiankou@gmail.com (V. Tatsiankou).

participating instruments are calibrated against the WSG and produce the new national or institutional DNI references with traceability to the WRR. Likewise, during the FRC, the measurements from a triad of Precision Filter Radiometers (PFRs) serve as the reference to the world's aerosol measuring community. More recently, the PMOD development of a Precision Solar Radiometer (PSR) has enabled spectral DNI comparisons to be performed (Gröbner et al., 2014). All these events at the WRC provide unique opportunities to assess the performance of novel devices against global references. Our solar spectral irradiance meter (SolarSIM) is a first instrument to participate in all three WRC comparisons.

The SolarSIM uses ground-based measurements to inform software algorithms for rapid resolution of the location-specific solar spectrum, total irradiance and atmospheric constituents. The SolarSIM works by measuring the solar spectral irradiance in six carefully chosen wavelength bands, using silicon photodiodes with rugged, hard coated bandpass filters,¹ to allow spectral reconstruction through parametrization of the major atmospheric processes, including aerosol extinction, ozone and water vapor absorptions (Tatsiankou et al., 2013; Tatsiankou et al., 2016). The direct sun version of the SolarSIM allows the user to resolve in the 280–4000 nm range the spectral AOD, PWV, atmospheric total column ozone, and ultimately compute the spectral and broadband DNI - thus providing data that typically requires five to seven commercial instruments. The ability to simultaneously obtain these solar and atmospheric parameters with only one instrument reduces cost, avoids diversity in data acquisition protocols and setup requirements, and so facilitates many research and commercial applications (Caballero et al., 2018; Rodrigo et al., 2017; Majumdar and Cunningham, 2017; Theristis et al., 2016; Fernández et al., 2016).

In this paper we perform a complete uncertainty analysis for all SolarSIM measurands. We first define the uncertainty of irradiance measurement for each of six SolarSIM channels, and then use these findings to derive the uncertainties of spectral and broadband DNI, spectral AOD, PWV and total column ozone. These results are compared to actual measurements from four SolarSIMs at the WRC during 28 September to 10 October 2015, which participated in the 12th IPC (DNI comparison), fourth FRC (AOD comparison), and first SRC (spectral DNI comparison). Additionally, the SolarSIMs' measurements of PWV content and total column ozone were compared against data from a co-located Cimel sun photometer and Brewer MkIII spectrophotometer, respectively.

2. Instrumentation setup

Four SolarSIMs with serial numbers SN102 and SN103 (D1 model), and SN112 and SN113 (D2 model), manufactured by Spectrafy Inc., were installed on the roof top of the WRC in Davos, Switzerland (46.81°N, 9.84°E) on 27 September 2015. The SolarSIM-D2 is a more rugged version of the SolarSIM-D1, designed to have an extended temperature range, lower power consumption, and improved internal humidity management. The SolarSIMs have a $\pm 2.5^\circ$ field of view with a 1° slope angle, conforming to the World Meteorological Organization (WMO) standard for radiometric measurements of DNI (WMO, 2008). The instruments were mounted on a Brusag sun tracker with a custom aluminum plate and bracket, as shown in Fig. 1. They were aligned normal to the sun using a reference pinhole on each SolarSIM enclosure and a three point adjustment method. Each SolarSIM was interfaced to a laptop via Spectrafy's COMBOX accessory, which provides power and RS-485 communication to the instrument. A specialized graphical user interface on the laptop enables data acquisition from each instrument every five seconds. It takes 500 ms for a SolarSIM to acquire and send the current values, ambient temperature and pressure, and internal temperature and humidity to the host for analysis. Depending on the



Fig. 1. SolarSIMs, versions D1 and D2, installed on a Brusag tracker on the roof top at the World Radiation Center, Davos, Switzerland (white finish - SolarSIM-D1, silver finish - SolarSIM-D2). (For interpretation of the references to color in this figure legend, the reader is referred to the web version of this article.)

hardware specifications, it takes a typical laptop about 100 ms to process the raw data into spectral products. Throughout this paper, SolarSIMs SN102, SN103, SN112, and SN113 are referenced as SSIM 1, SSIM 2, SSIM 3, and SSIM 4, respectively.

3. Measurement methodology overview

The SolarSIM measures the calibrated irradiance in six optical bands centered at 420, 500, 610, 675, 880, and 940 nm with full widths at half maxima of 10 nm. It also senses the ambient temperature, atmospheric pressure, and the device's internal temperature. These measurements are fed into our radiative transfer model to derive the spectral DNI and AOD in the 280–4000 nm range (with a 1 nm resolution), broadband DNI, total column ozone and PWV (Tatsiankou et al., 2016). The atmospheric parameterization follows a methodology similar to a Simple Model of the Atmospheric Radiative Transfer of Sunshine (SMARTS) (Gueymard, 1995, 2006). SMARTS methodology was chosen because it has been demonstrated to have robust performance and fast computational speed (Gueymard, 2008), and, hence, it was adapted in our architecture. The procedure for parameterizing the atmosphere from the SolarSIM measurements consists of the following steps:

1. Calibrate an instrument:
 - a. Determine the temperature coefficients for each channel.
 - b. Perform on-sun calibration against a reference spectroradiometer or a reference SolarSIM.
2. Acquire the current from six optical channels, ambient temperature and pressure, and the internal temperature.
3. Use our radiative transfer model to derive the spectral irradiance, the spectral AOD, DNI, total column ozone and PWV content:
 - a. Compute the zenith angle and the sun-earth distance using National Renewable Energy Laboratory's (NREL) solar position algorithm (Reda and Andreas, 2008).
 - b. Apply the sun-earth distance correction on the extraterrestrial solar spectrum from Gueymard (2004).
 - c. Calculate Rayleigh scattering and the transmittances from various atmospheric gases (CO₂, CH₄, O₂, NO₂) (Gueymard, 2006).
 - d. Determine the spectral AOD and its transmittance from the 420, 500, 675, and 880 nm channels (Tatsiankou et al., 2013).
 - e. Compute the total column ozone and its spectral transmittance from the 610 nm channel (Tatsiankou et al., 2013).
 - f. Calculate the PWV content and its spectral transmittance from the 940 nm channel (Tatsiankou et al., 2013).

¹ conform to MIL-C-48497A and MIL-STD-801F standards.

- g. Determine the spectral irradiance by applying the derived atmospheric constituents' transmittances to the extraterrestrial spectrum (Tatsiankou et al., 2013).
- h. Integrate the spectral irradiance to obtain the DNI.

The absorption coefficients and mixing ratios of the atmospheric gases used in our algorithm are taken from SMARTS under light pollution conditions (Gueymard, 2006), except for the carbon dioxide, whose mixing ratio is set to 400 ppmv.

4. Uncertainty analysis

We perform the uncertainty analysis for a SolarSIM by generally following the Guide to the Expression of Uncertainty Measurements (GUM) (JCGM, 2008). Our procedure can be summarized in five steps:

1. Determine the equation or functional relationship describing or approximating the measurand.
2. Identify the dominant sources of uncertainty associated with each variable in the measurement equation or functional relationship from step 1.
3. Determine standard uncertainty for each variable using either statistical methods (Type A uncertainty) or non-statistical methods (Type B uncertainty). Type A uncertainty is defined as the standard deviation of the data set as per Eq. (1)

$$\mu_A = \sqrt{\frac{\sum_{i=1}^n (X_i - \bar{X})^2}{n-1}}, \quad (1)$$

where μ_A is the Type A uncertainty, X_i are data points, \bar{X} is the mean of a data set, and n is the number of data points.

All other uncertainties that cannot be statistically estimated are labeled as Type B uncertainties, and are assumed to have either a rectangular or a normal distribution. These relationships are defined in Eqs. (2a) and (2b), respectively, as

$$\mu_{B,\text{rectangular}} = \frac{u_e}{\sqrt{3}}, \quad (2a)$$

$$\mu_{B,\text{normal}} = \frac{u_e}{k}, \quad (2b)$$

where $\mu_{B,\text{rectangular}}$ and $\mu_{B,\text{normal}}$ are the Type B uncertainties with a rectangular and a normal distribution, respectively, u_e is the uncertainty estimate, and k is a desired coverage factor.

For variables with multiple sources of uncertainties, we combine them using the Root Sum Squared (RSS) method.

4. Calculate the combined standard uncertainty of the measurand by adding standard uncertainties from step 3 using the RSS method.
5. Calculate the expanded uncertainty by multiplying the combined standard uncertainty by a desired coverage factor, k . In our case, we chose $k = 1$ to give the confidence level of 68%, as our combined standard uncertainty estimates are believed to be conservative.

Using this general procedure, we first evaluate the uncertainty of SolarSIM irradiance measurement in the six optical channels. For this case, the most dominant processes are identified as the on-sun calibration against a reference spectroradiometer and the photodiodes' temperature dependence. We then use these findings to estimate the uncertainty for our spectral model in deriving the spectral and broadband DNI, the spectral AOD, the total column ozone and PWV. We view the approach taken in this section as a good starting point in quantifying the uncertainties of numerous SolarSIM measurands. As more comparison data is gathered against reference instruments with well-defined uncertainties, a more refined estimate of the SolarSIM outputs' uncertainties will be obtained.

Table 1

Summary of the two main contributors to SolarSIM channel irradiance uncertainty. α is the photodiode temperature coefficient, μ_α is its standard uncertainty, and μ_t is the uncertainty of the temperature correction; μ_s is the uncertainty in the reference spectroradiometer's irradiance measurements. μ_t and μ_s are combined to yield μ_{irrad} , the combined standard uncertainty of irradiance measurement at each SolarSIM channel.

	Bandpass filter central wavelength, λ_c (nm)					
	420	500	610	675	880	940
Photodiode temperature response						
α (%/°C)	0.11	0.01	0.00	0.00	0.02	0.05
μ_α (%/°C)	0.019	0.008	0.011	0.012	0.009	0.017
μ_t (%)	0.44	0.20	0.25	0.28	0.21	0.39
Calibration uncertainties						
μ_s (%)	1.95	1.15	0.9	1.00	1.15	1.45
Combined irradiance uncertainties						
μ_{irrad} (%)	1.99	1.17	0.93	1.04	1.17	1.50

4.1. Temperature dependence

The spectral responsivity of silicon photodiodes varies as a function of temperature. The magnitude of this change is typically linear with temperature, and primarily depends on the silicon's crystal growth process, material quality, and packaging. Table 1 shows typical temperature coefficients for SolarSIM channels denoted by α , where %/°C is the percentage change of the photodiode responsivity per degree Celsius for the specific channel with a center wavelength, λ_c . The 500, 610, 675, and 880 nm channels exhibit negligible temperature dependence, while the 420 nm and 940 nm channels have a moderate temperature sensitivity of 0.11 and 0.05%/°C, respectively. We determine these coefficients by monitoring the photodiode outputs, during a temperature sweep under a 250 W quartz tungsten halogen light source. The spectral stability of the lamp is monitored by external silicon photodiodes with bandpass filters, whose center wavelengths and full-width at half-maxima are matched to the six SolarSIM channels. The SolarSIM's internal temperature is first cooled to 20 °C, then the device is placed on the thermo-electric cooler stage, which is pre-heated to 35 °C. We then gradually raise the temperature set point of the stage to 60 °C. As the internal temperature of the SolarSIM increases, we record the photodiode current from each channel versus the internal temperature. Once the internal temperature reaches 40 °C, we stop the test and compute the best line of fit slopes for each of the six channels, thereby yielding the temperature coefficients. We estimate the uncertainty of the temperature coefficient for each channel, μ_α , by computing the standard deviation, as per Eq. (1), of the derived temperature coefficients from ten experiments for the same device. We then define μ_t , the uncertainty in the temperature correction of the photodiode's responsivity

$$\mu_t = \frac{\mu_\alpha \cdot \Delta T}{\sqrt{3}}, \quad (3)$$

where ΔT is the maximum delta in °C the SolarSIM's internal temperature is assumed to undergo in the field as compared to the corresponding temperature during the optical calibration. We set ΔT as 40 °C. Eq. (3) has the square root of three in the denominator because we assume μ_t is a Type B uncertainty with a rectangular distribution. The computed values of μ_t for each channel are presented in Table 1.

4.2. On-sun optical calibration

The SolarSIM's optical channels have been calibrated for absolute irradiance, on-sun, against a LI-1800 secondary standard spectroradiometer at NREL. The calibration procedure ensures that the absolute irradiance measured by the SolarSIM in its six optical channels matches the irradiance as measured by the reference spectroradiometer at the corresponding wavelengths. By doing so, we largely compensate

for deviations from the filter transmittances and photodiode responsivities assumed in our spectral model, except for filter's center-wavelength and full width at half maxima variations from the nominal values. The dominant source of uncertainty in performing this procedure is the LI-1800's irradiance measurement uncertainty, μ_s , which has been quantified by NREL's researchers (personal communication with Afshin Andreas, September 2017). We combine μ_t and μ_s to yield

$$\mu_{\text{irad}} = \sqrt{\mu_t^2 + \mu_s^2}, \quad (4)$$

where μ_{irad} is the combined standard uncertainty of the SolarSIM irradiance measurement, as summarized in Table 1. Evidently, the measurement uncertainty of the reference spectroradiometer is a limiting component of the SolarSIM accuracy.

4.3. Spectral DNI uncertainty

We have estimated the combined standard percent uncertainty in deriving the spectral irradiance from the SolarSIM's radiative transfer model, $\mu(\lambda)_{\text{spec}}$, by comparing the spectral DNI as measured by the EKO's WISER spectroradiometer in the 350–1633 nm range against the corresponding spectra simulated by the SolarSIM's model. We define this uncertainty

$$\mu(\lambda)_{\text{spec}} = \sqrt{\mu_{\text{model}}(\lambda)^2 + \mu_{\text{wiser}}(\lambda)^2}, \quad (5)$$

where μ_{model} is the standard uncertainty of our model with respect to the WISER data and $\mu_{\text{wiser}}(\lambda)$ is the WISER's combined standard uncertainty, which we assumed as 2.5% across the entire spectral range. We calculate $\mu_{\text{model}}(\lambda)$ as

$$\mu(\lambda)_{\text{model}} = \sqrt{\frac{\sum_{i=1}^n [D_i(\lambda) - \bar{D}(\lambda)]^2}{n-1}} + \frac{\bar{D}(\lambda)}{\sqrt{3}}, \quad (6)$$

where $D_i(\lambda)$ is the percent spectral difference between simulated and measured spectra for timestamp t , $\bar{D}(\lambda)$ is the mean percent spectral difference of the entire data set, and n is the number of measured spectra. The first part of Eq. (6) is the standard deviation of the percent spectral difference between the measured and simulated spectra data set, while the second part is $\bar{D}(\lambda)$ which we treated as a Type B component with a rectangular distribution. We included the latter component in the uncertainty calculation because it cannot be compensated for during the optical calibration.

Over 10,000 WISER spectra were gathered from 19 September 2014 to 17 March 2015, when the WISER was in spectral DNI mode at the Solar Radiation Research Facility (SRRL) (Andreas and Stoffel, 1981). The data set was filtered to exclude cloudy periods by only accepting spectra when the DNI is over 300 W/m². We simulated the variability in bandpass filter transmittances by applying the center-wavelength's manufacturing tolerance of ± 2 nm to the nominal filter transmittance using a rectangular distribution. The corresponding filter profiles and photodiode responsivities were superimposed with the measured spectral DNI from the WISER spectroradiometer to simulate a distribution of theoretical currents from each SolarSIM channel, similar to the technique used in our previous work (Tatsiankou et al., 2013). In addition, we applied the combined standard uncertainty, μ_{irad} , with normal distribution from Table 1 to the simulated current values to mimic realistic in-field operation. Local ambient temperatures and atmospheric pressures were also extracted from the SRRL database and fed into the SolarSIM model for each five minute interval. Fig. 2 shows the computed mean percent spectral difference and the percent spectral standard deviation of the analyzed data set, as well as, μ_{spec} , the combined standard uncertainty of our model in deriving the spectral DNI. Based on this analysis, we then split the spectral uncertainty into three ranges: < 420 nm, 420–880 nm, > 880 nm, and assign conservative combined standard uncertainties of < 10%, < 3%, and < 5%, respectively, as per Fig. 2. Note that we have not included data corresponding to the oxygen absorption peaks centered at 687 and 761 nm, and water

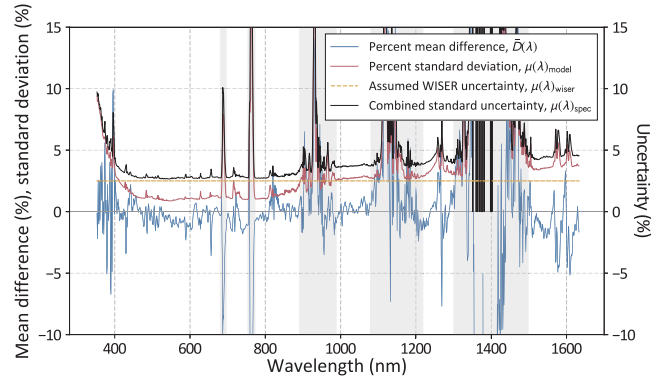


Fig. 2. The estimated spectral uncertainty of our model as compared to the spectral DNI measurements from NREL's EKO WISER spectroradiometer. Over 10,000 measured spectra was used in this analysis. We assume the WISER has a flat 2.5% spectral measurement uncertainty across its 350–1633 nm range. The mean percent difference, the percent standard deviation, and the estimated combined uncertainty of our spectral DNI model was derived by comparing the simulated and measured spectra. The gray areas denote the oxygen absorption peaks centered at 687 and 761 nm, and water vapor absorption bands centered at 934, 1130, and 1400 nm, where increased uncertainty is expected.

vapor absorption bands centered at 934, 1130, and 1400 nm. In those areas we expect increased uncertainty due to the extreme gradients of numerous oxygen and water vapour absorption lines. We have applied the computed uncertainties from the three ranges to the AM1.5D spectrum and computed the absolute spectral DNI uncertainty in units of W/m²/nm for each range, as shown in Table 3.

4.4. DNI uncertainty

We have estimated the combined standard uncertainty, in units of W/m², for the SolarSIM's DNI measurement, μ_{DNI} , by performing a comparison of the DNI data generated by the SolarSIM-D2 SN107² against the two first class CHP-1 pyrhemeters from Kipp and Zonen at the SRRL. We define this uncertainty through the following expression

$$\mu_{\text{DNI}} = \sqrt{\mu_d^2 + \mu_{\text{chp}}^2}, \quad (7)$$

where μ_{chp} is the combined standard uncertainty of the CHP-1 pyrhemeters, assumed as 10 W/m², and μ_d is the uncertainty of the SolarSIM SN107 DNI data versus reference DNI data. We express μ_d as

$$\mu_d = \sqrt{\frac{\sum_{i=1}^n (d_i - \bar{d})^2}{n-1}} + \frac{\bar{d}}{\sqrt{3}}, \quad (8)$$

where d_i is the DNI difference in W/m² between the SolarSIM and pyrhemeters for data point i , \bar{d} is the mean difference of the SolarSIM versus the reference DNI data set, and n is the number of analyzed data points per instrument. The first part of Eq. (8) is the standard deviation of the DNI difference between the SolarSIM's and reference instrument's data sets, while the second part is \bar{d} , which we treated as a Type B component with a rectangular distribution. We included the latter component in the uncertainty calculation because it cannot be compensated for during the optical calibration.

The comparison spanned the entire year from 2 September 2016 to 2 September 2017, with data being filtered to exclude cloudy periods as in previous section. Over 100,000 cloud-free data points per instrument are used in the analysis with a one minute resolution. The reference DNI data was obtained by averaging the values from both CHP-1 pyrhemeters. The mean difference and the standard deviation of the SolarSIM's DNI values as compared to the CHP-1 pyrhemeters' data are -1.6 W/m² and 8.3 W/m², respectively. We then computed the

² SolarSIM-D2 SN107 data is publicly available at http://midcdmz.nrel.gov/srri_ssim/.

combined standard uncertainty of the SolarSIM SN107 DNI measurement to be 13.0 W/m^2 as per Eq. (7), or 1.5%, as the mean reference DNI was 869.9 W/m^2 . We assume the estimated DNI uncertainty is valid for all SolarSIMs.

4.5. AOD uncertainty

The SolarSIM determines the spectral AOD in the 280–4000 nm range using four wavelength bands: 420, 500, 675, and 880 nm. These four channels create three aerosol regimes (below 500 nm, between 500 and 675 nm, and above 675 nm) within which the SolarSIM algorithm assumes that AOD behaves according to the Ångström power law. We assume the standard uncertainty in the AOD derivation, μ_{AOD} , depends primarily on the uncertainties of the spectral irradiance measurement, μ_{irrad} , and the assumed irradiance of the AM0 spectrum in each aerosol channel, μ_{AM0} , and can be expressed as

$$\mu_{\text{AOD}} = \sqrt{\mu_{\text{irrad}}^2 + \mu_{\text{AM0}}^2} \quad (9)$$

We assume that other uncertainties, such as calculation of the total ozone column, Rayleigh scattering, and optical air masses, are much smaller compared to the aforementioned ones. The uncertainty of irradiance measurement in the four aerosol channels is detailed in Table 1. The uncertainty of the AM0 irradiance in the four aerosol channels is estimated from Gueymard (2004). In that work the standard deviation of the integrated irradiance for the 400–700 nm and 700–1000 nm bands was found to be 1.2% and 0.8%, respectively. We then combine μ_{irrad} and μ_{AM0} as per Eq. (9) and summarize the results in Table 2. We extend the analysis to the 280–4000 nm range from the computed AOD channel uncertainties. For wavelengths below 420 nm and above 880 nm, we estimate the uncertainties by combining the AOD uncertainties at 420 and 500 nm, and 675 and 880 nm channels, respectively, using the RSS method. For the 420–500 nm, 500–675 nm, and 675–880 nm ranges, the AOD uncertainty is conservatively estimated to be the largest uncertainty of the two channels bounding the spectral region, as shown in Table 3. We find the lowest AOD uncertainty of 0.014, for an air mass of 1, to be in the 675–880 nm region.

4.6. Precipitable water vapour uncertainty

We have estimated the combined standard uncertainty, in units of mm, for the SolarSIM's PWV measurement, $\mu_{\text{H}_2\text{O}}$, similar to Section 4.4. We compared the PWV data derived by SolarSIM-D2 SN107 against the co-located PWV reference at the SRRL - Zephyr Geodetic Global Position System (GPS) Antenna and a Trimble Net9R Data Acquisition system. We express $\mu_{\text{H}_2\text{O}}$ as

$$\mu_{\text{H}_2\text{O}} = \sqrt{\mu_{\text{h}}^2 + \mu_{\text{GPS}}^2}, \quad (10)$$

where μ_{h} is the uncertainty of the SolarSIM's PWV data with respect to the reference PWV data, with the latter having an estimated combined standard uncertainty, μ_{GPS} , of 1 mm (Andreas and Stoffel, 1981). The expression for μ_{h} is defined by Eq. (8), where d_i is the PWV difference, in units of mm, between the SolarSIM and the reference instrument for data point i , \bar{d} is the mean PWV difference of the SolarSIM versus the

Table 2

The combined standard uncertainty of retrieving the AOD, μ_{AOD} , at four SolarSIM's aerosol channels, λ_i . μ_{AOD} primarily depends on the uncertainties in irradiance measurement and the AM0 spectrum, μ_{irrad} and μ_{AM0} , respectively.

λ_i (nm)	μ_{irrad} (%)	μ_{AM0} (%)	μ_{AOD} (%)	μ_{AOD}^a
420	1.99	1.2	2.32	0.023
500	1.17	1.2	1.68	0.017
675	1.04	0.8	1.31	0.013
880	1.17	0.8	1.41	0.014

^a For an air mass of 1.

Table 3

The summary of relative and absolute combined standard uncertainties for SolarSIM outputs, which include the spectral DNI and the AOD in the 280–4000 nm range, the broadband DNI, the ozone and PWV amounts.

Parameter	Range (nm)	Uncertainty (%)	Absolute uncertainty
Spectral DNI	<420	<10	<0.099 $\text{W/m}^2/\text{nm}^*$
	420–880	<3	<0.043 $\text{W/m}^2/\text{nm}^*$
	>880	<5	<0.044 $\text{W/m}^2/\text{nm}^*$
	280–4000	1.5	13.0 W/m^2
AOD**	<420	2.9	0.029
	420–499	2.3	0.023
	500–675	1.7	0.017
	675–880	1.4	0.014
	>880	1.9	0.019
PWV	N/A	14.6	1.6 mm
Ozone	N/A	18.8	64 DU ^a

* At AM1.5D conditions.

** For an air mass of 1.

reference PWV data set.

Analogously to Section 4.4, the PWV comparison spanned the entire year from 2 September 2016 to 2 September 2017. Over 100,000 cloud-free data points per instrument are used in the analysis with a one minute resolution. The mean difference and the standard deviation of the SolarSIM's PWV values as compared to the reference instrument's data are -0.94 mm and 1.08 mm , respectively. We then compute the combined standard uncertainty of the SolarSIM-D2 SN107's PWV measurement to be 1.57 mm as per Eq. (10), or 14.6%, as the mean PWV reference value was 10.76 mm . We assume the computed PWV uncertainty is valid for all SolarSIMs.

4.7. Ozone column retrieval uncertainties

At the time of writing, there was no available long term data comparing the total column ozone derived from a SolarSIM-D2 and a reference ozone instrument, such as the Brewer spectrophotometer. As such, we use a non-standard technique of estimating the ozone retrieval uncertainty of the SolarSIM. We simulate the spectral DNI with SMARTS under AM1.5D conditions (using an ambient pressure of 101.325 kPa, an airmass of 1.5, an AOD at 500 nm of 0.084, an ozone content of 340 DU, and a PWV of 14.2 mm). We then reconstruct the SMARTS spectrum using our six channel spectral model by applying the irradiance uncertainty to the optical channels as per Table 1 and AM0 uncertainties from Table 2, assuming a normal distribution. In addition, we simulate the variability in bandpass filter transmittances by applying the manufacturer's center wavelength tolerance of $\pm 2 \text{ nm}$ to the nominal filter profile using a rectangular distribution. The retrieved ozone values are compared to SMARTS's nominal ozone input of 340 DU. Consistent results are achieved by analyzing 10,000 spectra, and we obtain a mean difference of 2 DU and a standard deviation of 64 DU. We combine these quantities as per Eq. (8), where d_i is the total ozone column difference in units of DU between the SolarSIM's derived ozone content and the SMARTS's input of 340 DU for iteration i and \bar{d} is the mean total ozone column difference of the data set. The results yield the SolarSIM's combined standard uncertainty for total column ozone as 64 DU or 18.8%.

5. Performance at the World Radiation Center

5.1. WMO International Pyrheliometer Intercomparison XII

The WMO International Pyrheliometer Intercomparison (IPC) was first held in 1959 and now takes place every five years at the WRC in Davos, Switzerland. The IPC ensures traceability of the solar radiation measurements through the World Radiometric Reference (WRR), which

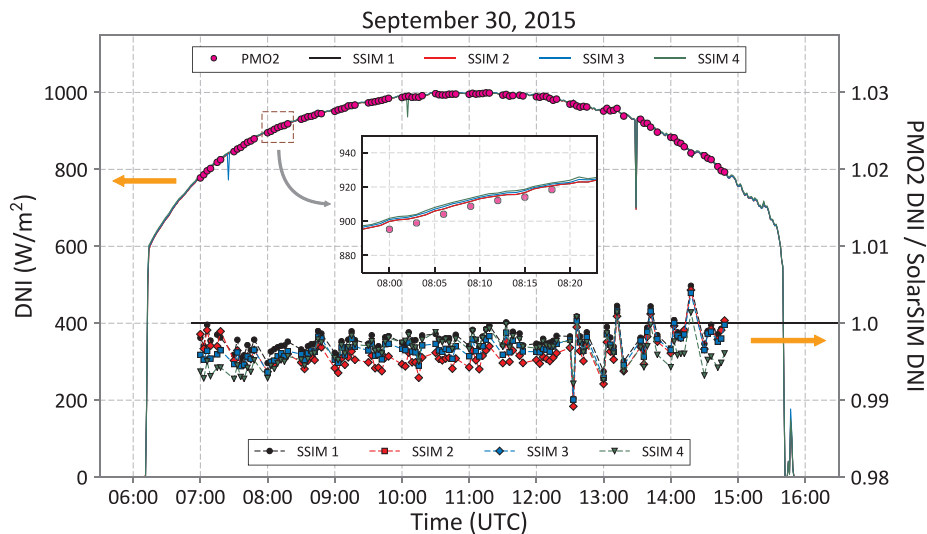


Fig. 3. A comparison of the daily DNI (left axis) and the ratio of the DNI (right axis) as measured by the IPC reference instrument (PMO2) and the SolarSIMs on September 30, 2015. The inset is the DNI profile magnification from 07:55 to 08:25 UTC.

is the world standard for total solar irradiance. The WRR is determined from the irradiance average of six absolute cavity radiometers: CROM2L, MK67814, HF18748, PAC3, PMO2, and PMO5, otherwise known as the World Standard Group (WSG).

The IPC-XII (2015) attracted 111 attendees from 33 countries and 134 new WRR factors were determined for participating radiometers, including the four SolarSIMs previously described (Finsterle, 2016). PMO2 absolute cavity radiometer with the correction factor to the WRR served as the DNI reference during the event. DNI measurements were conducted in periods of 19.5 min duration, re-starting every 30 min. The base cadence was one irradiance measurement every 90 s, which resulted in a maximum of 14 irradiance readings per series from the PMO2, assuming acceptable atmospheric conditions (data were discarded if the AOD at 500 nm exceeded 0.12). DNI data from each SolarSIM were submitted daily to the WRC for evaluation.

Fig. 3 shows the daily DNI profiles as resolved by the SolarSIMs and the reference absolute cavity radiometer on 30 September 2015. The latter is represented by the solid (magenta) dots, and the former are shown by the four lines; the inset provides a magnified comparison of the absolute DNI values. Note the SolarSIM’s DNI data was averaged over ± 15 s from a minute mark, and then this value was assigned to that minute. The ratios of the IPC reference DNI and the SolarSIMs’ DNI fall within $\pm 1\%$. The average ratio between the IPC reference and the test instrument define the WRR factor for the latter. The WRR factors for the SolarSIMs as computed by the WRC are 0.999674, 0.998951, 0.994610, and 0.99949, with standard deviations of 0.14%, 0.22%, 0.2%, and 0.25% for SSIM 1, SSIM 2, SSIM 3, and SSIM 4, respectively (Finsterle, 2016).³ These results are consistent with the DNI uncertainty analysis conducted in Section 4.4.

5.2. Spectroradiometer comparison

The First Spectroradiometer Comparison at the WRC included three types of spectral measurement equipment: one EKO MS711/MS712 (WISER) spectroradiometer, two Precision Solar Radiometers (PSRs) (Gröbner et al., 2014), and four SolarSIMs. The main specifications of these instruments are presented in Table 4. Due to the limited spectral range of the PSRs and the WISER, the spectral comparison was restricted to the 300–1700 nm range. October 1, 2015 was selected for the analysis because data from all participating instruments were available.

³ The IPC-XII report mentions COFOVO Energy as the manufacturer of the SolarSIMs. Since then, the SolarSIM business has been transferred to Spectrafy Inc.

Table 4

Specifications of the three types of instruments participating in the First Spectroradiometer Comparison.

Manufacturer	Instrument	Resolution	Step	Range
WRC	PSR	1–6 nm	0.7 nm	302–1020 nm
EKO	WISER	7 nm	1 nm	300–1700 nm
Spectrafy	SolarSIM-D2	1 nm*	1 nm*	280–4000 nm*

* Based on a spectral reconstruction model.

The timestamps from every instrument were synchronized to the nearest minute, resulting in 66 matching spectra between 09:00 and 15:00 UTC. The average DNI spectra for all seven instruments are presented in Fig. 4a. The spectral irradiance data from the SolarSIMs have been smoothed using a 5 nm central averaging technique, to better match the lower spectral resolution of the spectroradiometers. Fig. 4b shows the mean spectral difference and spectral standard deviation for the SSIM 1 versus the PSR-004 over the 302–1020 nm range, and versus the EKO WISER over the 1021–1700 nm range. The standard deviation mainly falls within the uncertainties for spectral DNI as presented in Table 3, except for areas below 315 nm and above 1650 nm. For the first range, the SolarSIM’s short wavelength extrapolation of the AOD from 420 nm and 500 nm channels is the most likely cause. For the latter range, the WISER is known to have problems with order sorting filters (Andreas, 2016). Nonetheless, the mean difference of the spectral DNI between the SolarSIMs and the reference spectroradiometers was < 5%, excluding the oxygen and PWV bands. The statistical performance of SSIM 1 is representative of the other three SolarSIMs.

5.3. Filter Radiometer Comparison IV

The Filter Radiometer Comparison (FRC) is held with the same regularity as the IPC. The FRC-IV attracted over 30 AOD-resolving instruments belonging to AERONET, GAW-PFR, Skynet, SURFRAD and other measurements networks. The instruments included Spectrafy’s SolarSIM, WRC’s Precision Filter Radiometer (PFR) and Precision Solar Radiometer (PSR), Middleton Solar’s SP02, Cimel’s CE318, Yankee Environmental System’s Multi-Filter Rotating Shadow-band Radiometer, Prede’s POM-2, and Microtops’ model II hand-held sun photometer (Schmutz et al., 2016).

One of the main goals of the FRC is to homogenize the global AOD measurements through traceability to the world’s aerosol standard group of spectral radiometers. This standard is defined as a triad of

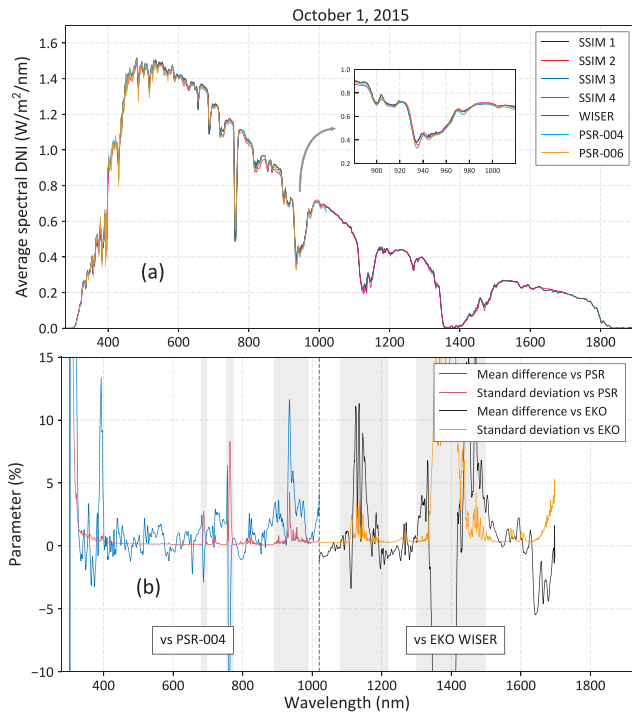


Fig. 4. (a) The average spectral DNI of 66 time-synchronous spectra from each of four SolarSIMs, two PSRs, and the EKO WISER spectroradiometer at the WRC from 09:00 to 15:00 UTC on October 1, 2015. The inset is the magnification for the 881–1020 nm spectral range. (b) The mean difference, standard deviation, and the combined uncertainty of the spectral DNI between the SolarSIM SN102 and PSR-004, EKO WISER spectroradiometers on October 1, 2015. The analysis spanned the 302–1020 nm and 1021–1700 nm ranges for the PSR-004 and EKO WISER, respectively. The gray areas denote the oxygen absorption peaks centered at 687 and 761 nm, and water vapour absorption bands centered at 934, 1130, and 1400 nm, where increased standard deviation is expected. Note that SolarSIM data were smoothed with 5 nm central averaging to aid comparison.

reference PFR instruments, which is established by the World Optical Depth Research and Calibration Center at the WRC, and is based on the recommendation from the WMO (Kazadzis et al., 2017). Each PFR measures the AOD at 368 nm, 412 nm, 500 nm, and 862 nm with a $\pm 1.25^\circ$ field of view and a 0.7° slope angle.

Since the SolarSIM resolves in real time the complete AOD spectrum across the 280–4000 nm range, comparisons were made against all four PFR channels. Fig. 5 shows a full day of time-synchronous AOD differences between the SolarSIMs and PFR triad data obtained on 30

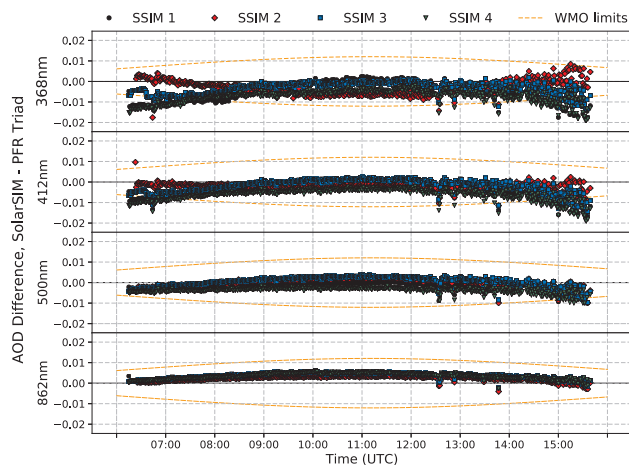


Fig. 5. AOD difference comparison between the SolarSIMs and the PFR triad for data acquired on 30 September 2015.

September 2015. The dashed orange lines delimit the AOD differences according to the WMO recommended U_{95} criterion, defined as (WMO, 2005)

$$U_{95} < \pm [0.005 + 0.01/m], \quad (11)$$

where m is the optical air mass. The first term accounts for instrumental and algorithmic uncertainties, while the second term addresses the relative uncertainty in instrument calibration. The U_{95} criterion stipulates that the AOD measured by high quality instruments should be within the specified limits 95% of the time.

As is evident from Fig. 5, the AOD differences between the SolarSIMs and the PFR triad at 500 nm and 862 nm are consistently within the U_{95} limits for most of the day. At 368 nm and 412 nm, however, the AOD differences tends to be lower than the U_{95} limit at air masses of greater than 3.5 or at sun elevation angles less than 16° , which correspond to measurement times before 07:00 UTC and after 15:20 UTC. Most likely, the differences in the AOD retrieval algorithms, such as the calculation of air mass, Rayleigh scattering, and ozone absorption, and differences in calibration methods between the instruments are responsible for these AOD discrepancies. The PFR triad has maintained a stability of under 1% since 2005. This is achieved by continuous monitoring of the differences of the three instruments and six month periodic checks using transferable instruments that are calibrated by the Langley technique at Izaña Atmospheric Observatory in Spain and Mauna Loa Observatory in USA. SSIM 1 and SSIM 2 were calibrated against a Licor LI-1800 secondary standard spectroradiometer at the NREL in Golden, US, while SSIM 3 and SSIM 4 were calibrated against SSIM 1 at the SUNLAB Solar Test Site in Ottawa, Canada (Tatsiankou et al., 2016). The latter method is expected to have higher uncertainty in the AOD measurement as compared to the Langley plot method.

The aggregate AOD performance of all SolarSIMs from 28 September to 1 October 2015 is summarized in Table 5, where λ , $\Delta\tilde{\mu}$, σ , and $N_{U_{95}}$ denote the AOD wavelength, the median AOD difference, the standard deviation of the AOD difference, and the percentage of data points that fall within the U_{95} criterion, respectively. The data statistics are generated for two SolarSIMs' calibrations performed against the PGS-100 and LI-1800 spectroradiometers, respectively, at NREL. PGS-

Table 5

Summary of the SolarSIMs' AOD performance against the PFR triad from September 28 to October 1, 2015, where λ , $\Delta\tilde{\mu}$, σ , and $N_{U_{95}}$ denote the AOD wavelength, the median AOD difference, the standard deviation of the AOD difference, and the percentage of data points that fall within the WMO's U_{95} criterion, respectively. Data are presented for two different calibrations - against the PGS-100 and LI-1800 spectroradiometers deployed by the National Renewable Energy Laboratory. Note, the italicised values denote the SolarSIM's AOD wavelengths for which less than 95% of data points fall within the WMO criterion from Eq. (11).

λ	Device	Calibration vs. PGS-100		Calibration vs. LI-1800	
		$\Delta\tilde{\mu} \pm \sigma$	$N_{U_{95}}(\%)$	$\Delta\tilde{\mu} \pm \sigma$	$N_{U_{95}}(\%)$
368 nm	SSIM 1	+ 0.027 ± 0.010	8.6	-0.001 ± 0.006	85.7
	SSIM 2	+ 0.020 ± 0.005	0	-0.002 ± 0.004	97.8
	SSIM 3	+ 0.018 ± 0.007	13.3	-0.002 ± 0.003	95.1
	SSIM 4	+ 0.026 ± 0.010	8.8	-0.006 ± 0.005	79.5
412 nm	SSIM 1	+ 0.014 ± 0.006	32.9	-0.001 ± 0.004	92.9
	SSIM 2	+ 0.011 ± 0.005	38.1	-0.000 ± 0.002	99.1
	SSIM 3	+ 0.010 ± 0.005	66.6	-0.000 ± 0.003	97.1
	SSIM 4	+ 0.011 ± 0.006	46.8	-0.005 ± 0.004	85.2
500 nm	SSIM 1	-0.000 ± 0.003	100.0	-0.001 ± 0.002	98.9
	SSIM 2	+ 0.001 ± 0.005	99.9	+ 0.002 ± 0.003	99.2
	SSIM 3	+ 0.000 ± 0.004	100.0	+ 0.002 ± 0.003	99.3
	SSIM 4	-0.004 ± 0.005	100.0	-0.003 ± 0.002	97.9
862 nm	SSIM 1	-0.005 ± 0.003	100.0	+ 0.004 ± 0.002	99.6
	SSIM 2	-0.004 ± 0.005	100.0	+ 0.003 ± 0.002	99.4
	SSIM 3	-0.004 ± 0.004	100.0	+ 0.005 ± 0.002	99.4
	SSIM 4	-0.003 ± 0.004	100.0	+ 0.004 ± 0.003	99.2

100 has a non-removable collimation tube and hence cannot be directly calibrated using a standard lamp method. Instead, it is calibrated outdoors in the direct normal mode against the LI-1800 spectroradiometer, which results in higher measurement uncertainty for the PGS-100 as compared to the LI-1800. As a result, the AOD performance of the SolarSIMs is poorer when the PGS-100 calibration is applied as compared to a LI-1800 calibration, especially for < 420 nm. Nonetheless, the performance of all SolarSIMs for both calibration methods fall within the calculated uncertainties from Table 2. Furthermore, using the LI-1800 calibration for 500 nm and 862 nm all four SolarSIMs comply with the WMO U_{95} criterion, while for 368 nm and 412 nm two out of four SolarSIMs meet this criterion⁴. The short wavelength extrapolation, especially at 368 nm, is understandably slightly less accurate than the longer wavelength interpolations.

5.4. Precipitable water vapor content comparison

Precipitable water vapor (PWV) is a highly-variable trace gas in the atmosphere that serves as a key input parameter in weather predictions models and climate studies (Liang et al., 2015; Karabatić et al., 2011). During the IPC-XII, PWV data acquired by a co-located Cimel CE318 sun photometer from the Aerosol Robotic Network (AERONET) was compared against PWV data derived by the SolarSIMs (Holben et al., 1998). Both instruments measure the solar irradiance near 940 nm, which is well suited for analyzing the atmospheric PWV content according to Halthore et al. (1997).

Fig. 6 shows the daily profile of PWV content on 30 September 2015, as measured by the SolarSIMs and the Cimel CE318 sun photometer. The SolarSIMs, on average, report PWV values that are approximately 1 mm higher than the Cimel CE318. Extending the evaluation over a 13 day period, a comparison of the daily average PWV content is shown in Fig. 7. Over this time period 248 time-synchronous data points were gathered for the SolarSIMs and the Cimel, allowing the calculation of the mean differences and standard deviations of 0.96 ± 0.21 mm, 1.02 ± 0.23 mm, 0.71 ± 0.15 mm, and 0.84 ± 0.23 mm for SSIM 1, SSIM 2, SSIM 3, and SSIM 4, respectively; the average Cimel PWV was 5.72 mm. These results are in line with measurement uncertainties of both the SolarSIMs and the Cimel, considering the Cimel can have a measurement bias of -25% or -1.43 mm under these PWV conditions (Schneider et al., 2010). We view these comparative results as a good starting point in quantifying the PWV measurement accuracy of the SolarSIM. Future research will include a long-term, comparative study between a SolarSIM and a Fourier Transform Infrared Spectrometer to gain a further insight into the PWV retrieval capability of the SolarSIM.

5.5. Total column atmospheric ozone comparison

Ozone is an atmospheric gas critically necessary to attenuate solar UV radiation, which has been linked to skin cancer, immune system suppression, and eye damage (WHO, 1994). As a result, it is crucial to monitor the total column ozone in the atmosphere. At present, Brewer spectrophotometers comprise the largest ground-based ozone measurement network in the world, spanning 40 countries (Gao et al., 2010). However, the Brewer is an expensive instrument with involved measurement procedures (Karhu, 2016). In contrast, the SolarSIM infers the total ozone column from a channel at 610 nm, which is spectrally situated near the peak ozone absorption in the Chappius band (Tatsiankou et al., 2016). Because ozone absorption at 610 nm is weak, less than 6% at AM1.5D conditions, it is of interest to assess the accuracy of the SolarSIM-derived ozone data against the Brewer spectrophotometer.

During the IPC-XII, the Brewer MkIII #163 spectrophotometer was

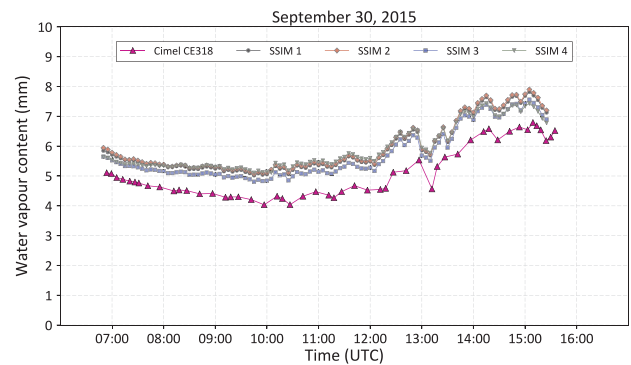


Fig. 6. Daily water vapor content profile as measured by the SolarSIMs and the Cimel CE318 sun photometer on September 30, 2015.

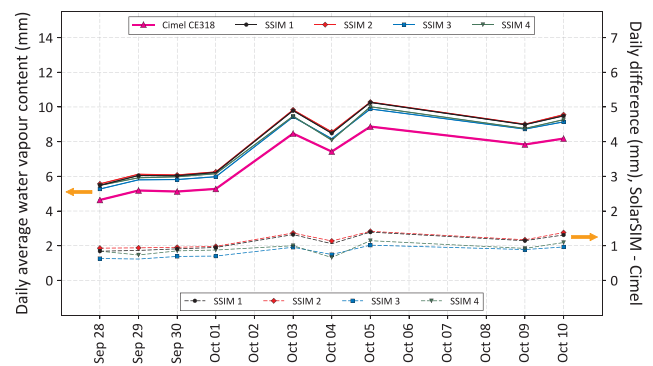


Fig. 7. Daily average water vapor content (left axis) and the difference in the daily water vapor content (right axis) as measured by the SolarSIMs and the Cimel CE318 sun photometer.

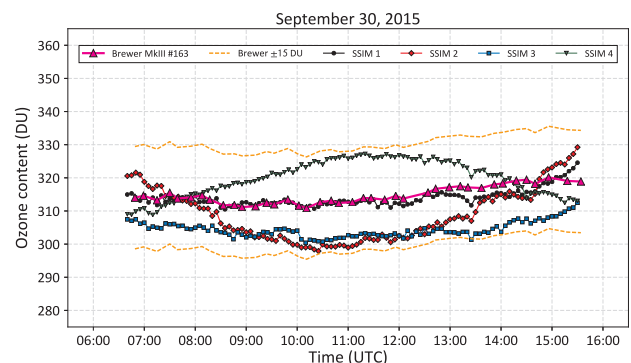


Fig. 8. The daily profile of the total ozone column amount as measured by the SolarSIMs and the Brewer MkIII spectrophotometer #163 on 30 September 2015.

in continuous operation at the WRC. The daily atmospheric ozone profiles as measured by the Brewer spectrophotometer and the SolarSIMs were compared, with data from 30 September 2015 shown in Fig. 8. The SolarSIMs' ozone measurements are all within ± 15 DU (or $\pm 5\%$) of the reference Brewer measurements. Further assessment was made over the course of two weeks, with 236 matching data points collected between all instruments, over 70% of them occurring between 28 September and 2 October 2015. SolarSIM data with AOD values at 500 nm above 0.12 were discarded, in compliance with the IPC criteria for determining adequate stability under cloudless conditions. For each day of testing, the daily ozone averages were computed for each device; comparisons with the Brewer spectrophotometer data are shown Fig. 9. The average of the daily differences between the SolarSIMs' and the Brewer and their standard deviations across the assessment period were -1 ± 5 DU, -4 ± 7 DU, -10 ± 8 DU, and 8 ± 7 DU for the SSIM 1, SSIM 2, SSIM 3, and SSIM 4, respectively; the average Brewer's total

⁴ The SolarSIM AOD performance may be further improved with Langley plot calibrations in suitable locations.

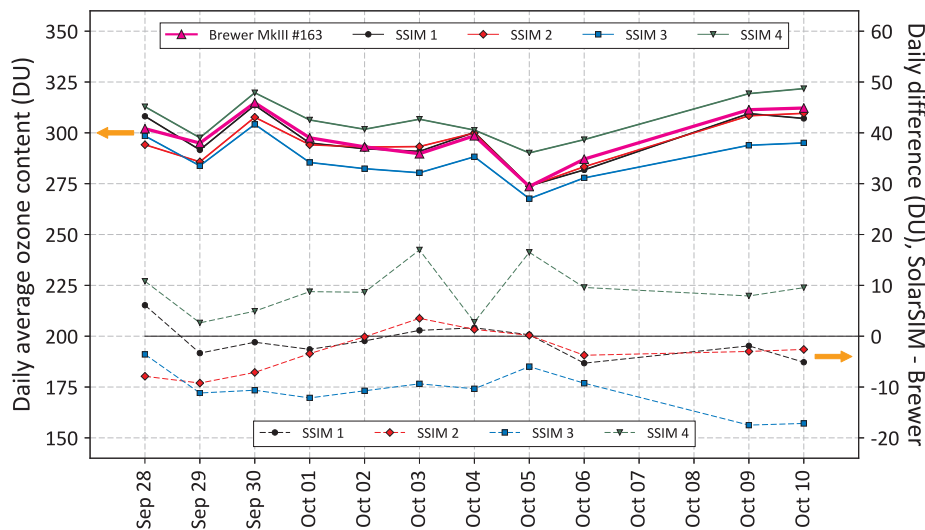


Fig. 9. A comparison of the daily average ozone content (left axis) and the daily average ozone difference (right axis) as measured by the SolarSIMs and the Brewer MkIII spectrophotometer 163 from 28 September 2015 to 10 October 2015.

ozone column was 300 DU. Multi-day measurements by the SolarSIMs apparently provide good quality ozone column data with much better performance than the estimated ozone retrieval uncertainty of 64 DU, as calculated in Section 4.7. However, the SolarSIM ozone measurements are very sensitive to small signal changes at 610 nm, which can occur due to misalignment or soiling. Since these data constitute “best-case” scenario, future research will include a long term study between SolarSIMs and Brewer spectrophotometers to gain further insights into the capability of SolarSIM to retrieve accurate total column ozone.

6. Conclusion

Measurements of direct sunlight are critical for numerous applications, including solar research, atmospheric science, and weather forecasting. Many commercial instruments, such as pyrheliometers, spectroradiometers, and sun photometers, exist for such purposes. Unlike these traditional instruments, the SolarSIM uses ground-based measurements in conjunction with a radiative transfer model to resolve in real-time broadband and spectral DNI, AOD, PWV and atmospheric total column ozone. We assessed the ability of the SolarSIM to resolve these parameters by first performing an extensive uncertainty analysis. These findings were then used to evaluate the measurements of four SolarSIMs deployed from 28 September to 10 October 2015 at the WRC. The availability of numerous, high-quality scientific instruments enabled further insight into the SolarSIM’s ability to resolve DNI, spectral DNI and AOD, atmospheric PWV content, and total column ozone.

The SolarSIMs’ DNI data were compared against the PMO2 absolute cavity radiometer from the WSG and the SolarSIMs were assigned the WRR factors ranging from 0.999674 to 0.994610. The mean difference in the spectral DNI between SolarSIMs and reference spectroradiometers was found to be < 5% for wavelengths above 400 nm. The median AOD differences and their standard deviations between the four SolarSIMs and the PFR triad averaged 0.0046 ± 0.0044 , 0.0016 ± 0.0034 , 0.0018 ± 0.0026 , and 0.0041 ± 0.0022 for 368 nm, 412 nm, 500 nm, and 865 nm, respectively. The mean difference in total column PWV and the corresponding standard deviation, as compared to a Cimel CE318 sun photometer, averaged 1 ± 0.2 mm for the four SolarSIMs. The difference in mean total column ozone and the corresponding standard deviation between the SolarSIMs and Brewer MkIII spectrophotometer averaged 6 ± 7 DU. The reported results were all within the estimated measurement uncertainties, albeit for the AOD and total column ozone the calculated uncertainties appear to be rather conservative. Therefore, further comparative studies are needed

to refine some of the uncertainties associated with the SolarSIM’s ability to resolve various atmospheric parameters.

Based on the presented data, we have shown that the SolarSIM-D2 is capable of performing accurate and precise measurements of broadband and spectral DNI, AOD, PWV, and total ozone column. Its compact size, low cost, and rugged design positions the SolarSIM-D2 as a potential alternative for routine and dependable monitoring of direct sunlight and atmospheric constituents. Further SolarSIM deployments and additional comparative studies against reference instruments will help determine the primary role of this promising device within the solar research and atmospheric science communities.

Acknowledgment

The authors would like to acknowledge support from the National Sciences and Engineering Research Council of Canada, the Ontario Research Fund - Research Excellence program, the Ontario Centres of Excellence, the Canada Research Chairs program, the Canadian Foundation for Innovation, and the National Research Council’s Industry Research Assistance Program.

We would like to thank Roberto Galleano from the Joint Research Center and Lionel Doppler from the German Meteorological Service for providing the spectral data, and Luca Egli from the World Radiation Center for sharing the ozone data. We also would like to acknowledge the NREL’s Solar Radiation Research Laboratory for providing the spectral and irradiance data sets used in our uncertainty analysis.

References

- AlYahya, S., Irfan, M.A., 2016. Analysis from the new solar radiation atlas for Saudi Arabia. *Solar Energy* 130, 116–127.
- Andreas, A., 2016. WISER Calibration Certificate at NREL < http://www.nrel.gov/aim/Calibrations/Spectral/MS7XX/7XX_2016_09.rpt.zip > .
- Andreas, A., Stoffel, T., 1981. NREL Solar Radiation Research Laboratory (SRRL): Baseline Measurement System (BMS). Golden, Colorado (Data); NREL Report No. DA-5500-56488.
- Araki, K., Yamaguchi, M., 2003. Influences of spectrum change to 3-junction concentrator cells. *Solar Energy Mater. Solar Cells* 75, 707–714.
- Caballero, J.A., Fernández, E.F., Theristis, M., Almonacid, F., Nofuentes, G., 2018. Spectral corrections based on air mass, aerosol optical depth, and precipitable water for PV performance modeling. *IEEE J. Photovolt.* 8 (2), 552–558.
- Cebecauer, T., Suri, M., 2016. Site-adaptation of satellite-based DNI and GHI time series: Overview and SolarGIS approach. In: AIP Conference Proceedings. AIP Publishing, pp. 150002.
- Fernández, E.F., Soria-Moya, A., Almonacid, F., Aguilera, J., 2016. Comparative assessment of the spectral impact on the energy yield of high concentrator and conventional photovoltaic technology. *Solar Energy Mater. Solar Cells* 147, 185–197.
- Finsterle, W., 2016. WMO International Pyrheliometer Comparison IPC-XII Final Report.

- WMO/IOM 124.
- Gao, W., Schmoldt, D., Slusser, J.R., 2010. UV Radiation in Global Climate Change: Chapter 6. Springer.
- Gröbner, J., Kouremeti, N., Nevas, S., Blattner, P., 2014. Characterisation Studies of Precision Solar Spectroradiometer. Technical Report. WRC/PMOD.
- Gueymard, C., 1995. SMARTS2: A Simple Model of the Atmospheric Radiative Transfer of Sunshine: Algorithms and Performance Assessment. Florida Solar Energy Center Cocoa, FL.
- Gueymard, C.A., 2004. The sun's total and spectral irradiance for solar energy applications and solar radiation models. *Solar Energy* 76, 423–453.
- Gueymard, C.A., 2006. SMARTS2 code, Version 2.9.5, User's Manual, Technical Report. Solar Consulting Services.
- Gueymard, C.A., 2008. Prediction and validation of cloudless shortwave solar spectra incident on horizontal, tilted, or tracking surfaces. *Solar Energy* 82, 260–271.
- Halthore, R.N., Eck, T.F., Holben, B.N., Markham, B.L., 1997. Sun photometric measurements of atmospheric water vapor column abundance in the 940 nm band. *J. Geophys. Res.* 102, 4343–4352.
- Holben, B., Eck, T., Slutsker, I., Tanre, D., 1998. AERONET - a federated instrument network and data archive for aerosol characterization. *Rem. Sens. Environ.* 66, 1–16.
- Holben, B., Tanre, D., Smirnov, A., Eck, T., 2001. An emerging ground-based aerosol climatology: aerosol optical depth from AERONET. *J. Geophys. Res.: Atmos.* 106, 12067–12097.
- JCGM, 2008. Evaluation of Measurement Data - Guide to the Expression of Uncertainty in Measurement. Bureau International des Poids et Mesures.
- Karabatić, A., Weber, R., Haiden, T., 2011. Near real-time estimation of tropospheric water vapour content from ground based GNSS data and its potential contribution to weather now-casting in Austria. *Adv. Space Res.* 47, 1691–1703.
- Karhu, J.M., 2016. Brewer spectrometer total ozone column measurements in Sodankylä. *Geoscient. Instrumen., Meth. Data Syst.* 5, 229.
- Kazadzis, S., Kouremeti, N., Gröbner, J., 2016. Fourth WMO Filter Radiometer Comparison (FRC-IV).
- Kazadzis, S., Kouremeti, N., Nyeki, S., Gröbner, J., Wehrli, C., 2017. The World aerosol Optical depth Research and Calibration Center (WORCC), Quality assurance and quality control of GAW-PFR AOD measurements. *Geoscient. Instrumen., Meth. Data Syst. Disc.* 2017, 1–19.
- Liang, H., Cao, Y., Wan, X., Xu, Z., Wang, H., Hu, H., 2015. Meteorological applications of precipitable water vapor measurements retrieved by the national GNSS network of China. *Geod. Geodynam.* 6, 135–142.
- Majumdar, Z.K., Cunningham, D.W., 2017. Performance metrics and testing of micro-concentrated and hybrid photovoltaic systems for ARPA-E MOSAIC. In: *Optics for Solar Energy*. Optical Society of America, p. RW3B-2.
- Núñez, R., Domínguez, C., Askins, S., Victoria, M., Herrero, R., Antón, I., Sala, G., 2016. Determination of spectral variations by means of component cells useful for CPV rating and design. *Prog. Photovolt.: Res. Appl.* 24, 663–679.
- Reda, I., Andreas, A., 2008. Solar Position Algorithm for Solar Radiation Applications. Technical Report. NREL.
- Rodrigo, P.M., Fernández, E.F., Theristis, M., Cruz, F.A., 2017. Characterization of the spectral matching ratio and the z-parameter from atmospheric variables for CPV spectral evaluation. *IEEE J. Photovolt.* 7, 1802–1809.
- Schmutz, W., Finsterle, W., Kazadzis, S., Kouremeti, N., Gröbner, J., Thomann, C., 2016. PMOD Annual Report 2015.
- Schneider, M., Romero, P., Hase, F., Blumenstock, T., Cuevas, E., Ramos, R., 2010. Continuous quality assessment of atmospheric water vapour measurement techniques: FTIR, Cimel, MFRSR, GPS, and Vaisala RS92. *Atmos. Measur. Techniq.* 3, 323–338.
- Tatsiankou, V., Hinzer, K., Muron, A., Mohammed, J., Wilkins, M., Haysom, J., Schriemer, H., Myrskog, S., 2013. Reconstruction of the solar spectral resource using limited spectral sampling for concentrating photovoltaic systems. In: *Photonics North*. International Society for Optics and Photonics.
- Tatsiankou, V., Hinzer, K., Schriemer, H., Haysom, J.E., Beal, R., 2016. Design principles and field performance of a solar spectral irradiance meter. *Solar Energy* 133, 94–102.
- Theristis, M., Fernández, E.F., Almonacid, F., Pérez-Higueras, P., 2016. Spectral corrections based on air mass, aerosol optical depth, and precipitable water for CPV performance modeling. *IEEE J. Photovolt.* 6, 1598–1604.
- WHO, 1994. Ultraviolet Radiation, vol. 160. World Health Organization.
- WMO, 2005. Experts Workshop on a Global Surface Based Network for Long Term Observations of Column Aerosol Optical Properties, Technical Report. GAW Report 162.
- WMO, 2008. Guide to Meteorological Instruments and Methods of Observation.